Available online at www.sciencedirect.com

SciVerse ScienceDirect

Physics Procedia 34 (2012) 114 – 118

Physics Procedia

Simulating self-assembly with simple models

D. C. Rapaport

Department of Physics, Bar-Ilan University, Ramat-Gan 52900, Israel

Abstract

Results from recent molecular dynamics simulations of virus capsid self-assembly are described. The model is based on rigid trapezoidal particles designed to form polyhedral shells of size 60, together with an atomistic solvent. The underlying bonding process is fully reversible. More extensive computations are required than in previous work on icosahedral shells built from triangular particles, but the outcome is a high yield of closed shells. Intermediate clusters have a variety of forms, and bond counts provide a useful classification scheme.

1. Introduction

Self-assembly at microscopic scales is a fascinating phenomenon with likely application to nanotechnology in general and medicine in particular. The fact that the shells of spherical viruses [1, 2] are able to grow *in vitro* [3, 4, 5] – a purely physical process free of the influence of genetic material – suggests the possibility of packaging therapeutic payloads for targeted delivery directly to the cell following the example set by viruses. Spontaneous self-assembly at molecular scales is subject to significant thermal noise that opposes the forces driving growth; this introduces considerations not encountered at the macroscopic scale. The details of supramolecular self-assembly are not readily observed directly, but to some extent this experimental shortcoming can be alleviated by molecular dynamics (MD) simulation. On the assumption that simplified models capable of capturing the essential details can be formulated, information can be obtained about the underlying processes that is otherwise inaccessible.

Early MD studies of this self-assembly problem [6, 7] were limited by available computational power and therefore focused on assembly in the absence of solvent, subject to the restriction that bonds, once formed, are unbreakable. This was followed by a more demanding MD study of reversible assembly, a more reasonable approach physically, but avoidance of kinetic traps required that smaller particle clusters be decomposed at regular intervals. Inclusion of an atomistic solvent became possible with increased computing resources; the solvent introduces a diffusive component to the otherwise ballistic particle motion, allows collision-induced breakup of clusters without them coming into direct contact, and serves as a heat bath for absorbing and redistributing energy released during bonding.

This approach, when applied to triangular particles [8, 9], leads to the conclusion that their self-assembly into 20-particle icosahedral shells proceeds via a cascade of reversible bonding steps, with a high yield of full shells and a clear preference for maximally-bonded intermediate structures. While it may appear paradoxical, the reversibility aids efficient self-assembly by eliminating bonds that would otherwise lead to incorrect growth. The present paper summarizes the recent extension of these simulations to larger shells containing 60 trapezoidal particles that have the structural form of T=1 viruses. A fuller account of this work will appear in due course [10].

Email address: rapaport@mail.biu.ac.il (D. C. Rapaport)

doi:10.1016/j.phpro.2012.05.018

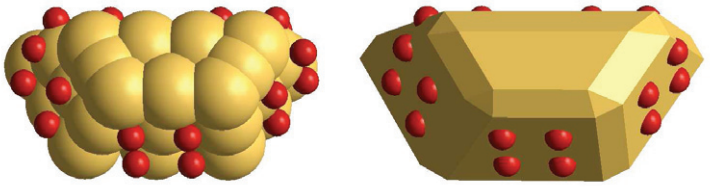

Figure 1: The trapezoidal particle showing the component soft spheres and the effective molecular shape; the small red spheres signify the attraction sites.

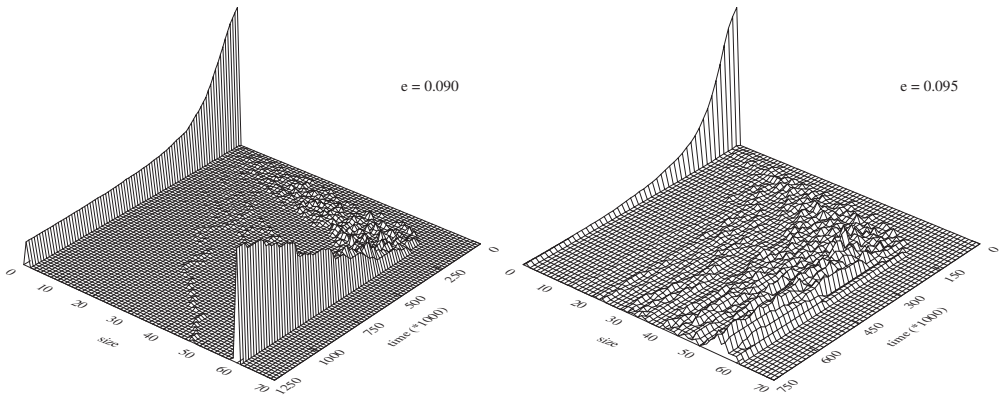

Figure 2: Time-dependent cluster size distributions expressed as mass fractions for two values of e; the final peaks for e=0.09 correspond to monomers and complete shells; each grid interval along the time axis (MD units) corresponds to $\sim 3 \times 10^6$ steps.

2. Methodology

The effective trapezoidal shape of the model capsomer particle, shown in Fig. 1, is obtained using a rigid assembly of soft-sphere atoms arranged so that 60 particles can be packed to form a closed polyhedral shell. Attractive forces act between pairs of interaction sites located on the lateral faces of the particles; these are responsible for bonding and help stabilize the complete shells, as well as ensuring that the assembly pathway leads to the correct structure. Bonding is reversible and, when sufficiently stretched, bonds will break. An explicit solvent, represented using soft-sphere atoms, is also included. Further details concerning the model, the motivation for the approach used, and the technical aspects of the MD simulations appear in [8, 9]. More general aspects of MD are covered in [11].

3. Results

The system contains a total of 125 000 trapezoidal particles and solvent atoms at an overall number density of 0.1; the particle concentration is 2.2%, enough for constructing 45 shells of size 60. Constant-temperature MD prevents heating due to exothermal bond formation. The strength of the attractive force is governed by a parameter e, and a series of runs covering a relatively narrow range of e values lead to a variety of outcomes that include no growth at lower e, high shell yield at slightly larger values, and no complete shells but a lot of partial assemblies as e is raised even further.

Fig. 2 shows examples of the time-dependent cluster-size distributions from two different runs; note the orientation of the plots aimed at revealing (for e=0.09) the near-absence of partial shells. The e=0.09 run produced the highest shell yield, 36 complete shells, amounting to 80% of the maximum possible, with just one incomplete shell of size 59, a smaller structure of size 48, and the remaining particles present as unbonded monomers. The other run shown

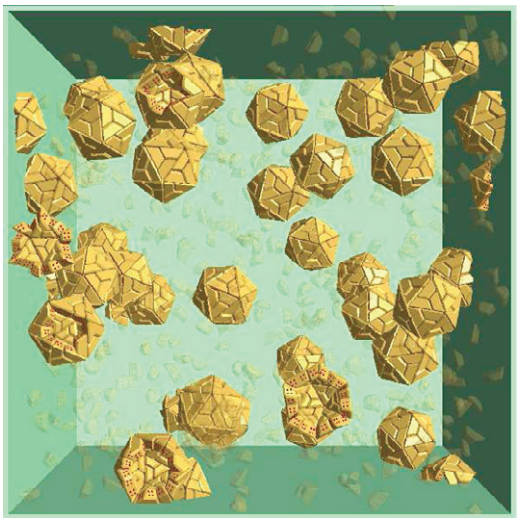

Figure 3: Final state of the e=0.09 run; solvent atoms are not shown and particles not in complete shells appear semitransparently (note that complete shells lying astride periodic boundaries can appear open – a visual artifact).

here is for e=0.095, where rapid early growth terminates prematurely due to exhaustion of the monomer supply. The image in Fig. 4 shows the e=0.09 run following completion of shell assembly.

The shell growth histories contain information about the intermediate structures unavailable using current experimental techniques. Given the wide range of possible partial assemblies that could eventually grow to form closed shells, it is important to devise schemes for extracting the essential features of such particle clusters. The variety is demonstrated in Fig. 4, where some of the growing shells (for e=0.09) are shown when they reach size 40. Images are recorded at the moment the cluster first reaches this size; most growth steps are in unit increments, but in two of the examples shown here the structure whose size is exactly 40 is skipped due to the partial shell bonding with a cluster of particles.

The most straightforward scheme for classifying intermediate structures is based on bond counts. For small and intermediate sizes, an increased bond count corresponds to geometrical compactness, whereas closer to completion it implies a reduced number of holes in what would otherwise be a full shell. Table 1 shows the observed bond-count spread for several cluster sizes and the frequency at which each occurs. The analysis is based on a large number of configuration snapshots over the entire e=0.09 run. Smaller clusters tend to achieve maximal or near-maximal bonding, while at intermediate and larger sizes this preference is somewhat reduced, but still clearly present. Loosely bound structures are entirely absent since thermal noise promptly detaches particles that fail to form multiple bonds.

A concise summary of all the bond count data over the range of sizes where the variation is significant appears in Fig. 5. The graph on the left shows the actual data, namely the minimum and maximum observed bond counts, the count ranges accounting for over 80% of cases, and the counts that occur most frequently. The maximum count grows approximately linearly with cluster size, with small deviations due to geometrical issues; the value spread for any given size is relatively small. An expanded view of the bond-count spreads appears in the graph on the right, in which the data is expressed as deviations from the maximum observed counts. Allowing for fluctuations, the spread grows until cluster size 50, and while in most cases the majority of the clusters tend to have bond counts that deviate by no more than 4 from the maximum, with the most frequent count lying just 1 or 2 below the maximum, the spread is broader in the size range 40-55.

This behavior is similar to the icosahedral shells considered previously [8] insofar as the smaller clusters are concerned, namely a strong preference for maximized bond counts. At intermediate sizes there is still a preference for a high degree of bonding, although less so than for the icosahedral case. The behavior differs as shells near completion; for the icosahedral case the observed maximal bond counts correspond to just a single opening in the shell, whereas with the larger shells there are often two or more holes. Shell size is only one factor governing the nature of the growth process; particle shape is also important, and the fact that trapezoidal particles can form multiple

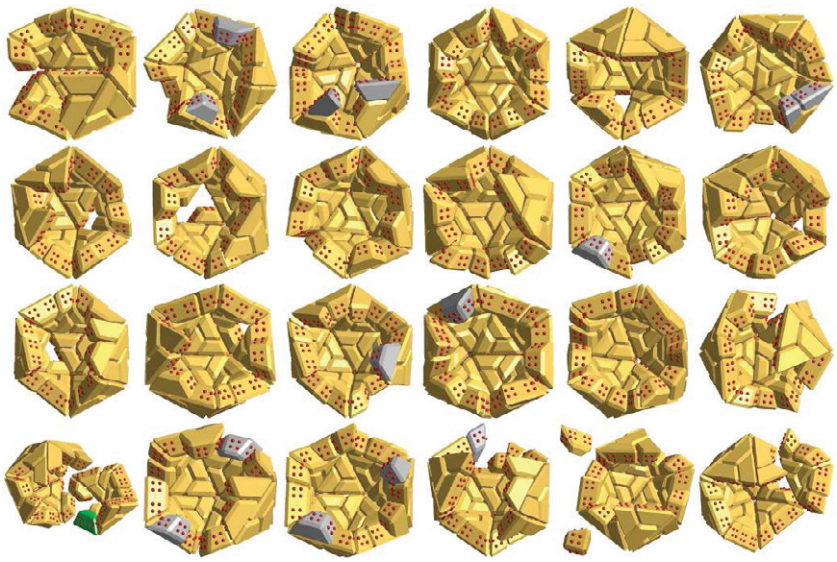

Figure 4: A selection of clusters of size 40 (with two exceptions – see text), each oriented for the best view of the outer boundary; color coding identifies particles belonging to the final shell into which the cluster develops (gold), those that will be subsequently expelled and not appear in the final shell (silver), and those belonging to another cluster about to bond with the one being tracked but also due to be expelled (green); other particles (with one exception) are excluded for clarity.

Table 1: Percentages of cluster realizations of size s having different bond counts b; the second column lists the ranges of b values observed for each s, and the remaining columns correspond to the b values in descending order; values below 10% are shown as '..' for clarity and the highest value is shown in bold.

s	b	Percentage														
5	7-6	**97**	..													
10	17-16	**96**	..													
15	28-24	21	**68**	..	..	..										
20	40-37	16	**35**	29	20											
25	52-47	14	20	**34**	11	17	..									
30	64-58	**31**	23	20	..	14	..	..								
35	76-71	12	15	**32**	15	15	12									
40	89-80	..	..	**53**	26	..	..	..	..	..	..					
45	102-93	13	10	..	**22**	10	14	14	..	..	..					
50	117-103	..	..	**23**	..	17	..	11	..	..	13	..	..	..	..	..
55	132-125	..	..	..	13	15	24	**31**	..							

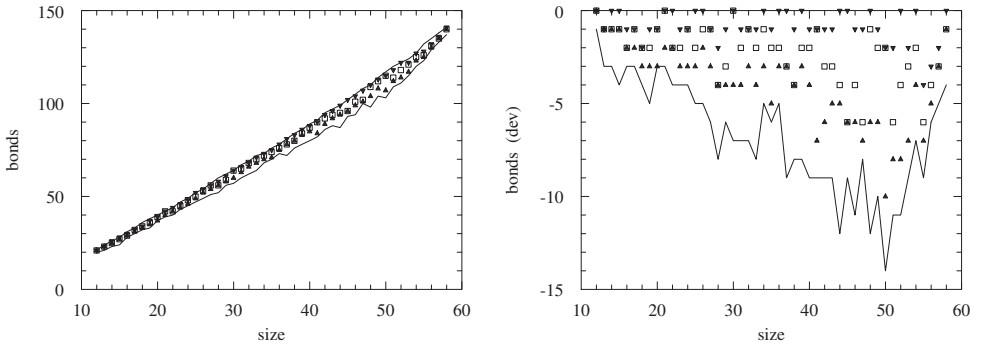

Figure 5: Bond counts and their deviations from the maximum observed counts for different cluster sizes; solid lines show the minimum and maximum counts, triangles the ranges accounting for over 80% of cases, and squares the most frequent counts.

bonds when attaching to a cluster (this is not always the case for triangular particles) reduces the need for the compact structures that aid in preventing bond breakage when triangular particles assemble.

Many other aspects of the behavior are revealed in the course of detailed analysis of the runs. Some of the features, such as the lifetimes of intermediate assemblies, or the probability of clusters of different sizes either growing or losing particles on account of reversible bonding, are amenable to quantitative study. Other features, exemplified by the morphologies of the intermediate states at a level beyond mere bond counts, or the nature of bonding events between extended clusters, require visualization in order to probe the details. These and other issues will be covered in a more extensive paper [10].

[1] F. H. C. Crick and J. D. Watson. The structure of small viruses. *Nature (Lond.)*, 177:473, 1956.
[2] D. L. D. Caspar and A. Klug. Physical principles in the construction of regular viruses. *Cold Spring Harbor Symp. Quant. Biol.*, 27:1, 1962.
[3] P. E. Prevelige, D. Thomas, and J. King. Nucleation and growth phases in the polymerization of coat and scaffolding subunits into icosahedral procapsid shells. *Biophys. J.*, 64:824, 1993.
[4] G. L. Casini, D. Graham, D. Heine, R. L. Garcea, and D. T. Wu. In vitro papillomavirus capsid assembly analyzed by light scattering. *Virology*, 325:320, 2004.
[5] A. Zlotnick and S. Mukhopadhyay. Virus assembly, allostery and antivirals. *Trends in Microbiol.*, 19:14, 2011.
[6] D. C. Rapaport, J. E. Johnson, and J. Skolnick. Supramolecular self-assembly: Molecular dynamics modeling of polyhedral shell formation. *Comp. Phys. Comm.*, 121:231, 1999.
[7] D. C. Rapaport. Self-assembly of polyhedral shells: A molecular dynamics study. *Phys. Rev. E*, 70:051905, 2004.
[8] D. C. Rapaport. Role of reversibility in viral capsid growth: A paradigm for self-assembly. *Phys. Rev. Lett.*, 101:186101, 2008.
[9] D. C. Rapaport. Modeling capsid self-assembly: design and analysis. *Phys. Biol.*, 7:045001, 2010.
[10] D. C. Rapaport. Molecular dynamics simulation of reversibly self-assembling shells in solution using trapezoidal particles. *arXiv:1201.2264*, 2012.
[11] D. C. Rapaport. *The Art of Molecular Dynamics Simulation*. Cambridge University Press, Cambridge, 2nd edition, 2004.